

# Development of Advanced Circulation Control Wing High-Lift Airfoils

Robert J Englar\* and Gregory G Huson†

*David Taylor Naval Ship Research and Development Center, Bethesda, Maryland*

Recent experimental and flight test programs have developed and confirmed the high lift capability of the Circulation Control Wing (CCW) concept. These CCW airfoils employ tangential blowing of engine bleed air over circular or near circular trailing edges and are capable of usable lift coefficients three times those of simple mechanical flaps. Earlier versions of these blown airfoils made use of relatively complex leading and trailing edge devices which would have to be retracted mechanically for cruise flight. In a continuing program to reduce the complexity, size, and weight of the CCW system, several series of advanced CCW airfoils have been developed which can provide STOL capability for both military and commercial aircraft using much smaller, less complex high lift systems. This paper will describe these configurations, present the experimental results confirming their aerodynamic characteristics, and also make comparisons with previous CCW and more conventional high lift systems.

## Introduction

THE development of high lift airfoils employing tangential blowing over round or near round trailing edges has been underway at David Taylor Naval Ship R&D Center since 1969.<sup>1</sup> Recent experimental and flight test programs<sup>2,5</sup> have confirmed the high lift and STOL capabilities of this Circulation Control Wing (CCW) concept. As applied to a typical fixed wing aircraft, the concept employs engine bleed air to pneumatically augment the wing's circulation lift and has generated section lift coefficients three times those of simple mechanical flaps. The application of this lift to provide STOL capability was flight verified<sup>3</sup> in 1979 when a rather large radius (0.0365 chord) CCW trailing edge was applied to the wing of a Navy/Grumman A 6 test bed aircraft. Figure 1 shows the wing fold airfoil section evaluated two dimensionally prior to the flight demonstrator development. Figure 2 records the increased lifting capability provided by the trailing edge blowing. The effectiveness of this round CCW trailing edge in augmenting wing lift resulted in significant STOL performance and heavy lift potential.<sup>4,6</sup> A demonstrated 140% increase in usable, trimmed lift coefficient produced reductions of 35% in approach speed, 60% in takeoff distance and 65% in landing ground roll relative to the standard A 6. Flight speeds as low as 67 knots were achieved by the A 6/CCW aircraft.

These flight results confirmed CCW as a simple and effective blown STOL system and also identified several improvements needed before the system could be incorporated into production aircraft. The large trailing edge radius demonstrated on the A 6/CCW aircraft ensured high lift augmentation but was not acceptable from a cruise drag standpoint. It would either have to be mechanically retracted or its size reduced to the point where the base thickness was no longer a penalty. A second problem area was the leading edge device required to prevent flow separation during the high circulation associated with STOL operation. Whereas the 37.5 deg slat deflection on the two dimensional model had proved sufficient, the flight demonstrator maximum deflection was mechanically limited to 25 deg. Therefore an

increased leading edge radius was added to the testbed aircraft and it performed quite satisfactorily. However for cruise flight it too would have to be retracted or the mechanical actuator/track system revised to allow greater deflection.

In order to address these areas of needed improvement a program has been underway since the flight test to develop advanced CCW airfoils by reducing the complexity, size, and weight of the CCW system without penalizing its lift augmenting capability. The program has two specific goals: 1) to develop an advanced CCW airfoil which would incorporate a smaller trailing edge blown plenum, and non-deflecting leading edge device (these would be within the contour of an existing supercritical airfoil which could replace current state of the art wing sections) and 2) to develop improved versions of CCW which are compatible with existing thin wings such as those already on the A 6 and other current high performance aircraft. In both cases, maintaining lift augmentation while reducing drag and complexity have been the dominant objectives of the program. The following sections will discuss the design considerations and experimental evaluations involved in the development of these airfoils and compare their performance to the earlier relatively complex CCW configurations.

## Design Considerations

### CCW/Supercritical Airfoil

It appeared that the above goals were attainable by taking advantage of the large leading and trailing edge thickness of a typical bluff trailing edge supercritical airfoil. Not only does this airfoil section geometry appear quite compatible with the incorporation of aft plenum, slot and small radius trailing edge, it also generates the improved transonic cruise performance afforded by increased critical Mach number and delayed drag rise. The developmental approach taken was to combine a typical proven supercritical section with a set of baseline CCW trailing edge parameters closely matching those of the A 6/CCW aircraft, and then experimentally evaluate the characteristics produced by progressively reducing the trailing edge size until it was compatible with the supercritical airfoil aft contour. The NASA 17% thick supercritical airfoil of Ref. 7 had been both wind tunnel and flight tested, and therefore had a suitable reference data base. The airfoil thickness produces a large bluff leading edge radius of 4.28% chord which is of such substantial size that it

Received June 26, 1982; revision received Jan. 10, 1983. This paper is declared a work of the U.S. Government and therefore is in the public domain.

\*CCW Program Manager, STOL Aerodynamics Group, Aircraft Division.

†Aerospace Engineer, STOL Aerodynamics Group, Aircraft Division, Member AIAA.

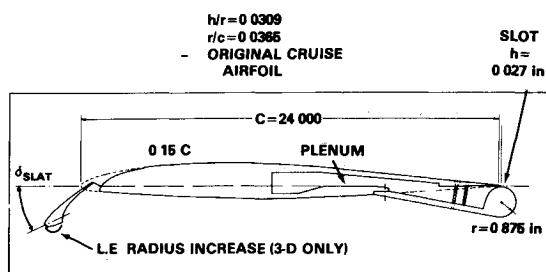


Fig 1 A 6/CCW wing fold airfoil section (64A008 4/CCW);  $\delta_{SLAT} = 37.5$  deg, large trailing edge radius

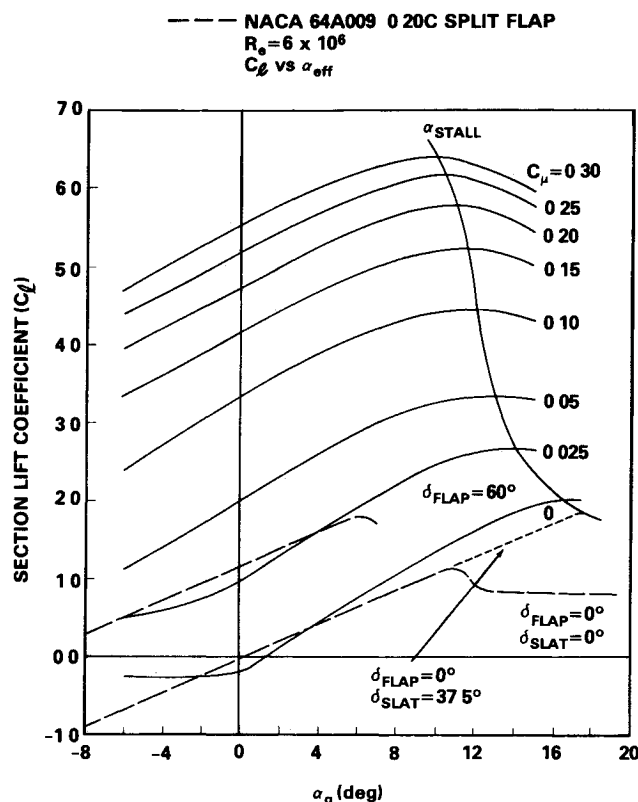


Fig 2 Lift characteristics of the 64A008 4/CCW airfoil;  $\delta_{SLAT} = 37.5$  deg,  $r/c = 0.0365$

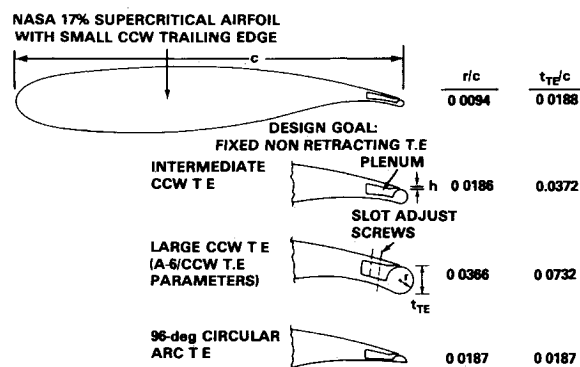


Fig 3 CCW/supercritical airfoil model geometries

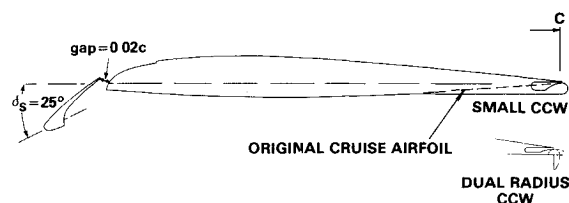


Fig 4 Incorporation of the small CCW geometries on the A 6/64A008 4 airfoil

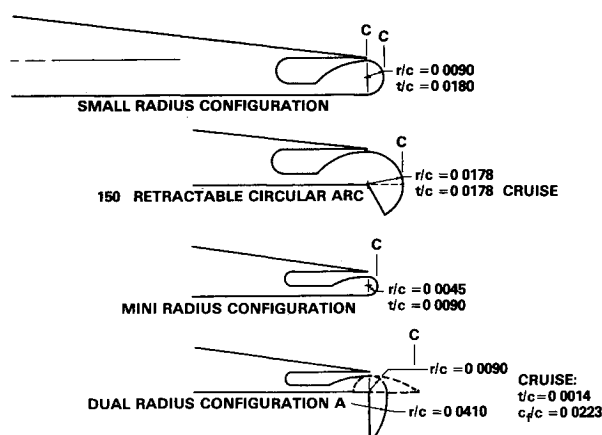


Fig 5 A 6/CCW small trailing edge detail and parameters

could substitute for a mechanical leading edge device and thus further simplify the high lift configuration. To parametrically vary the model trailing edge geometry the A 6/CCW design radius to chord ratio of 0.0365 was taken as a baseline reference value, halved to give  $r/c = 0.0186$  and halved again to give  $r/c = 0.0094$ . The smallest trailing edge diameter (0.0188c) is thus slightly greater than twice the 0.008c trailing edge thickness of the baseline supercritical airfoil. These model configurations are shown in Fig 3 where the pertinent CCW trailing edge parameters are also identified. The terms  $r$ ,  $h$ ,  $c$  and  $c$  represent trailing edge radius, jet slot height, original baseline airfoil chordlength, and effective airfoil chordlength including the radius, respectively. Since detailed discussion of the characteristics of these four airfoils is given in Refs 8 and 9 only the smallest radius configuration will be included in the following discussion of results.

#### A 6/CCW Airfoils

Because high performance aircraft typically employ thinner sections with sharp trailing edges, a second program was undertaken to extend the above smaller trailing edge

CCW/supercritical configurations to these thin airfoils. Because a data base was already established for the A 6 airfoil section it was selected as the reference thin airfoil. The 8.4% airfoil of Fig 1 was modified to accept the CCW trailing edges shown in Figs 4 and 5. The "small" radius ( $r/c = 0.009$ ) is the same trailing edge configuration used with the supercritical airfoil while the "mini" radius is half that size, yielding a cruise trailing edge diameter of 0.009c. Neither of these configurations is intended to be retracted in cruise, being one fourth and one eighth the size of the original flight test trailing edge. The retractable circular arc configuration uses a simple rotating segment to produce 150 deg of jet turning arc (as measured from the slot) when deflected for high lift, retracting to 96 deg and a trailing edge thickness of 0.0178c in cruise. The configuration thus has a cruise base thickness slightly less than the small round configuration but a radius approximately twice as large for effective jet turning. The dual radius configuration is in effect a very short chord (0.0223c) blown flap—with several important differences. It pivots about a lower surface hinge point with a radius the same as the above single radius configuration (0.009c), and deflects to 90 deg. The aft upper surface is not straight like the

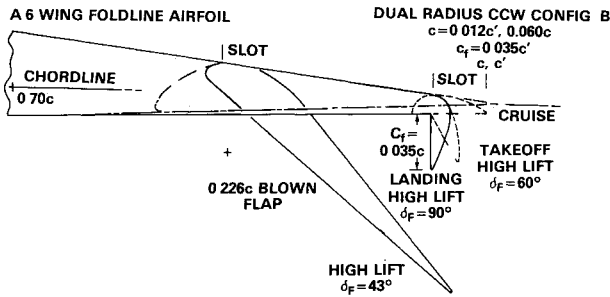


Fig 6 Dual radius CCW and blown flap configurations

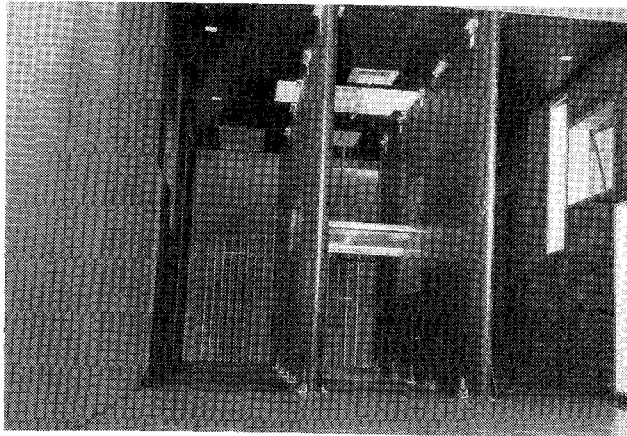


Fig 7 Airfoil installed in the DTNSRDC 3x8 ft subsonic two dimensional inserts

conventional blown flap, but is a second much larger radius, 0.041c. This produces a downstream CCW radius *larger* than the original flight demonstrator, but a cruise trailing edge thickness exactly the same as the clean A 6 airfoil, 0.0014c. The second radius adds additional jet deflection so that when the flap is deflected 90 deg, the jet angle is 122 deg from the slot. Jet attachment at this deflection should be enhanced by the larger radius. Two additional blown configurations were constructed and tested and are shown in Fig 6. The 0.226c blown flap is a Grumman Aerospace Corporation design<sup>10</sup> employing a straight aft upper surface with a radius downstream of the slot when the flap is deflected. A second dual radius CCW trailing edge, configuration B, has a larger flap chord than the first and is intended to produce more lift due to geometric camber when the blowing is off. Its radii are increased (because the hinge point moves forward) to 0.012 and 0.060c, but the cruise trailing edge thickness remains 0.0014c. Two additional deflection angles have been added: 0 deg (cruise) and 60 deg (intermediate lift at reduced drag, intended as a takeoff configuration). The jet turning angles for the 0, 60, and 90 deg flap deflections are thus 33, 93, and 123 deg respectively from the jet exit plane parallel to the chord.

Mention should be made of the design blowing momentum coefficient,  $C_{\mu}$  (to be defined in the following section). Expected full scale values are functions of bleed mass flow, available pressure and the flight velocity (a function of weight, incidence, lift coefficient obtained with blowing, and engine vertical thrust component). For the A 6/CCW flight demonstrator using existing bleed from its J 52 P8B turbojet engines, available  $C_{\mu}$  ranged up to 0.30. However, since current high performance aircraft may employ turbofan engines with less bleed capability, a limit on available momentum for these engines was estimated to yield  $0.05 < C_{\mu} < 0.15$ . Thus, for the majority of the thin airfoil small trailing edge data,  $C_{\mu}$  will be limited to approximately 0.17.

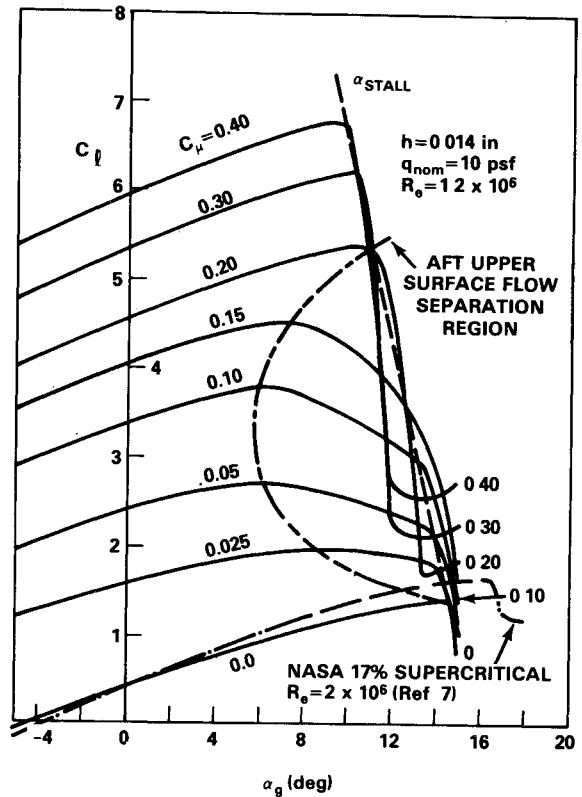


Fig 8 Variation in lift with incidence at constant blowing for the small trailing edge CCW/supercritical airfoil

### Experimental Apparatus and Technique

The 3 ft span, two dimensional models described above were mounted between the 3x8 ft subsonic two dimensional wall inserts installed in the DTNSRDC 8x10 ft subsonic tunnel (Fig 7). Lift and moment coefficients were obtained by numerical integration of surface static pressures near the midspan as recorded by a 144 port scanivalve system. The drag coefficient was obtained from integration of wake momentum deficit as measured on a fixed wake rake spanning nearly 8 ft from floor to ceiling. All reported force and moment coefficients are based on  $c$ , since this is considered to be the undeflected cruise reference chord. The value  $c'$  may differ from  $c$ , the original clean airfoil chord, in that the slot is located at the original airfoil trailing edge, and thus the new small CCW devices extend somewhat aft. The momentum coefficient  $C_{\mu}$  was calculated as  $\dot{m} V_j / (q c)$ , where  $\dot{m}$  is the mass flow per unit slot span as measured by venturimeter, and  $V_j$  is the isentropic jet velocity calculated from measured conditions using the equation in Ref 5. Model installation, test apparatus and technique, data reduction and corrections, and monitoring of tunnel two dimensionality were all conducted as reported in Ref 5 (Appendix A) and Ref 11.

### Results and Discussion

#### CCW/Supercritical Airfoil

The small radius configuration of Fig 3 was evaluated over a geometric angle of attack range  $-5 \text{ deg} \leq \alpha_g \leq +15 \text{ deg}$ . The relatively low freestream dynamic pressure of 10 psf ( $Re=1.2 \times 10^6$ ) yielded  $C_{\mu}$  values up to 0.40 instead of the 0.17 limit mentioned above. Lift data for a slot height of 0.014 in are presented in Fig 8 as functions of incidence and blowing. If these plots are compared to the state of the art A 6/CCW airfoil data of Fig 2 which was run at a larger slot height and Reynolds number, two trends are noticeable. First, the CCW/supercritical airfoil with a radius only 25% as large produces lift that is slightly greater than the A 6/CCW

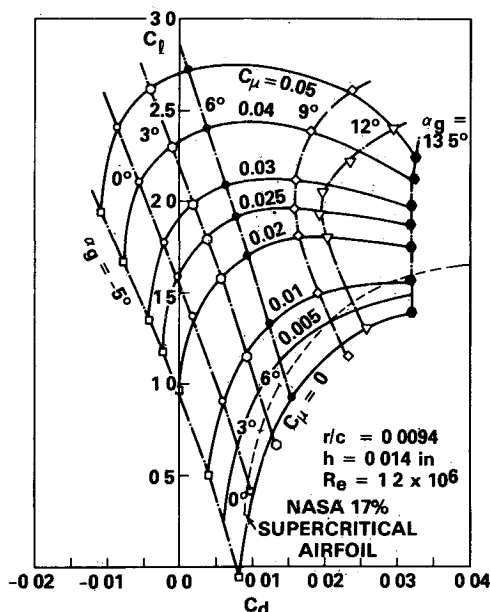


Fig 9 Drag polars for the small trailing edge CCW/supercritical airfoil at low blowing

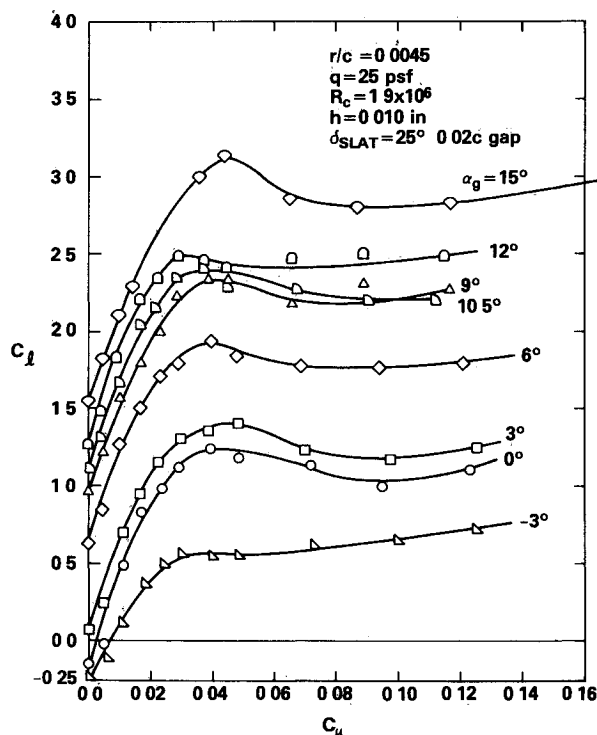


Fig 10 Lift due to blowing for the mini radius A 6/CCW airfoil

airfoil at low  $\alpha$  and  $C_\mu$ , since the A 6 slat imparts a download under these conditions. Second, the undeflected bulbous nose of the supercritical airfoil provides the same or better leading edge performance as the A 6 model's 37.5 deg slat, yielding almost identical stall angle at any given  $C_{lmax}$ .

The apparent deficits in certain of the lift curves (primarily for  $6 \text{ deg} \leq \alpha_g \leq 12 \text{ deg}$  and  $C_\mu < 0.20$ ) are due to flow separation on the supercritical airfoil cambered aft upper surface between the crest and the slot. (This condition is discussed in Ref. 12 and is not a leading edge separation.) The separated flow is re-entrained at higher  $C_\mu$ , and the deficits disappear. The same correction should occur at higher Reynolds numbers.

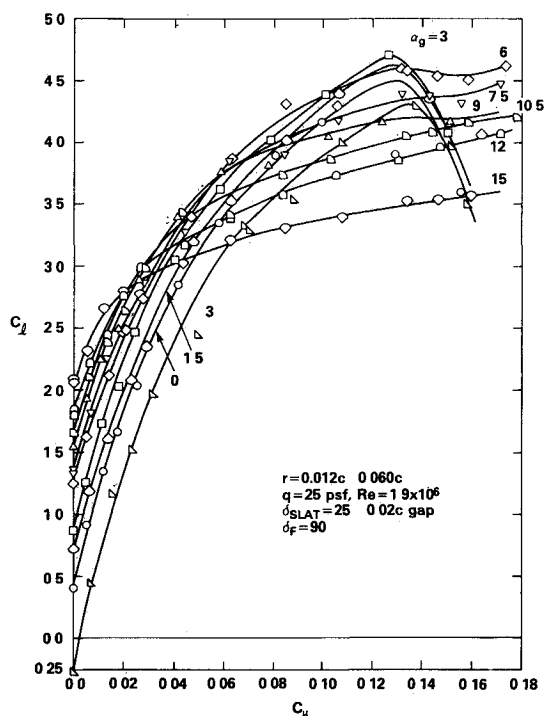


Fig 11 Lift due to blowing for dual radius configuration B;  $c_f = 0.035c$ .

Table 1 Comparison of unblown drag coefficient

Airfoil	$C_l$	$C_d$	$\alpha_g$ , deg
643 418	0.40	0.0063	0.7
Baseline supercritical	0.40	0.0084	0.0
Small CCW, $r/c = 0.0094$	0.40	0.0087	-0.7
Large CCW, $r/c = 0.0366$	0.40	0.0145	-3.7

Drag polars for the small radius airfoil at low blowing values are compared in Fig. 9 with the baseline 17% supercritical airfoil. The drag values of the baseline airfoil are slightly lower than those of the CCW/supercritical airfoil with no blowing ( $\Delta C_d = 0.0006$  at  $\alpha_g = 0 \text{ deg}$ ); however, the drag of the CCW airfoil can be reduced to that of the baseline airfoil by blowing at  $C_\mu \leq 0.003$  at typical values of cruise incidence. Additional blowing will reduce the drag even further, but an analysis of engine thrust loss due to required bleed should be considered. For  $Re = 2 \times 10^6$  and a typical cruise  $C_l$  of 0.4, unblown drag values for the small radius and a larger radius CCW/supercritical airfoil are compared with both the baseline supercritical and a typical sharp trailing edge airfoil in Table 1. At equal cruise lift, the drag of the baseline and small CCW airfoil is nearly equal. Thus, the high lift device of the small CCW/supercritical airfoil may be left exposed for cruise conditions with essentially no subsonic drag penalty.

#### A 6/CCW and Blown Flap Airfoils

##### Lift Generation

The various CCW and blown flap configurations of Figs. 4 and 6 were evaluated extensively over a range of subsonic dynamic pressures, angle of attack, and jet slot height. The data comparisons which follow are intended primarily to show the effect of configuration geometry changes on lift augmentation in the moderate blowing range of  $C_\mu < 0.17$ . It should be noted that while the original large radius A 6/CCW was tested with a 37.5 deg slat deflection (in order to keep flow attached at high circulation levels associated with  $C_\mu$  up to 0.30), the majority of the current tests were conducted with a

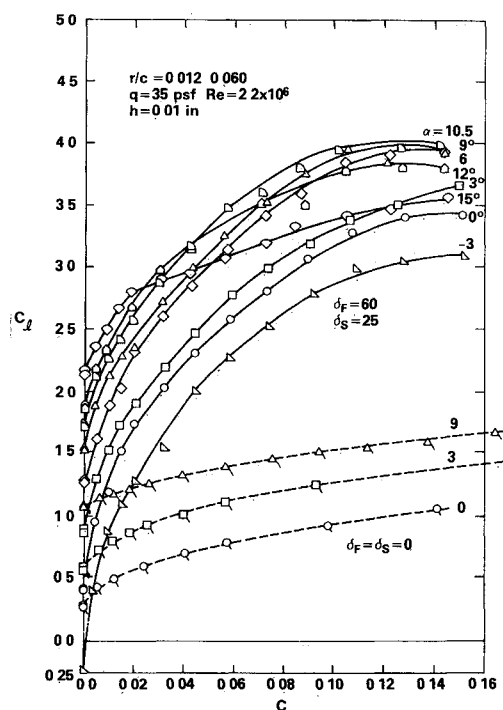


Fig 12 Lift due to blowing for dual radius configuration B;  $\delta_F = 0$  and 60 deg

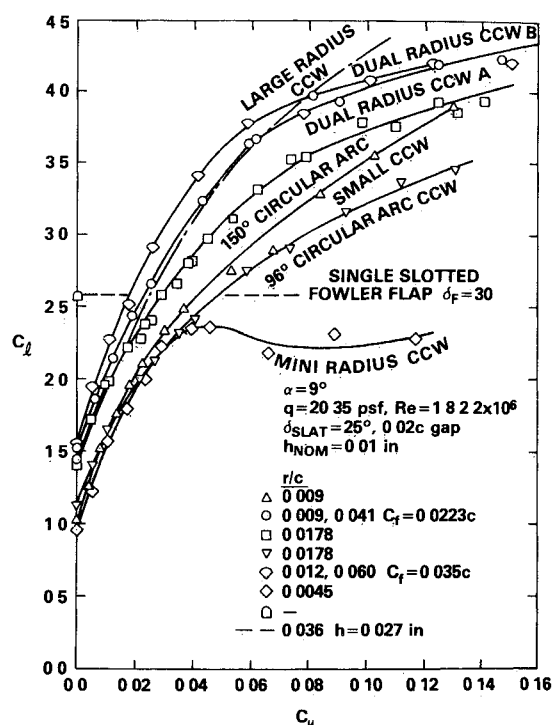


Fig 14 Comparative blown lift configurations;  $\alpha_g = 9$  deg

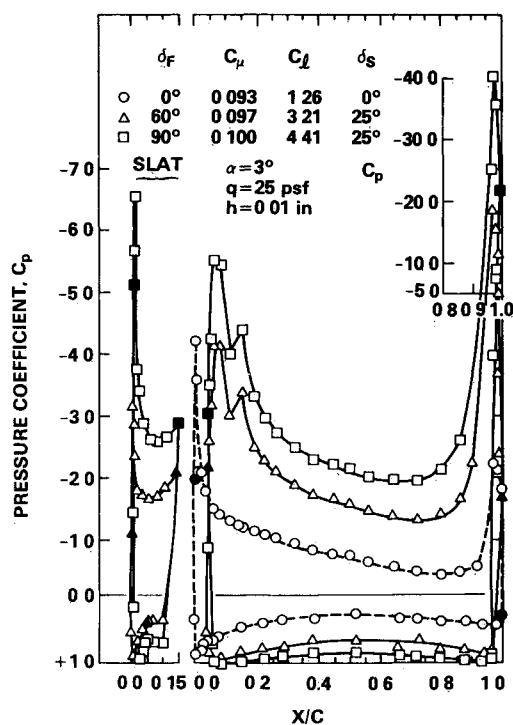


Fig 13 Pressure distributions for dual radius configuration B;  $c_f = 0.035c$

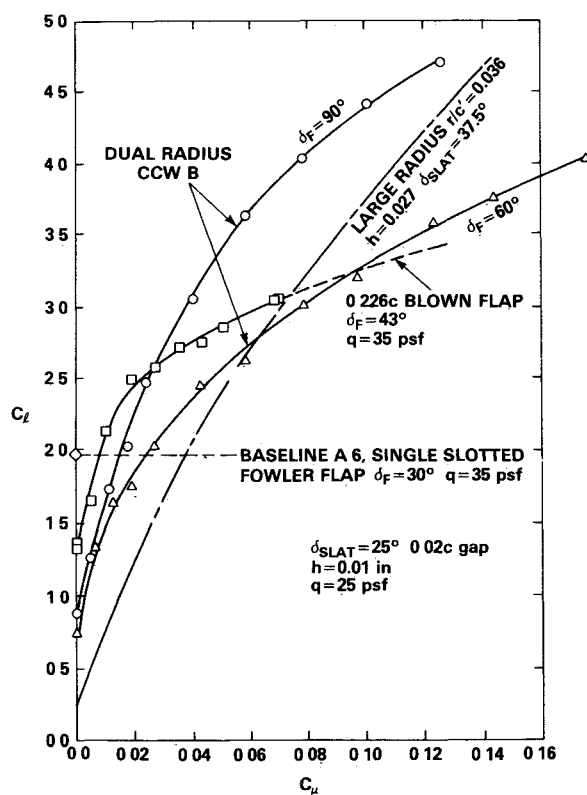


Fig 15 Comparative lift capability;  $\alpha_g = 3$  deg

slat deflection of 25 deg and a 0.02c gap. This is the slat setting on the production A 6 and it was originally thought to be more appropriate for the lower blowing levels. This choice did not prove appropriate in certain cases, as will be discussed later.

Lift resulting from blowing at constant geometric angle of attack is shown in Figs 10 and 11 for the two extremes in trailing edge radius size: 0.0045c for the mini radius configuration, and 0.060c for the larger radius of the dual radius configuration B airfoil. For the smallest radius (Fig

10), lift maxima occur at about  $C_\mu = 0.04$ , and augmentation beyond that is reduced. This same trend was noted in Refs 8 and 9 for the small radius supercritical airfoil once certain pressure ratios were exceeded. In Fig 10 that pressure ratio for the mini radius is about 1.4 to 1.5, but the ratio was considerably higher for the CCW/supercritical section with twice the radius. It becomes apparent that higher pressure ratios combined with smaller radii are not conducive to increased jet turning and lift augmentation. The favorable

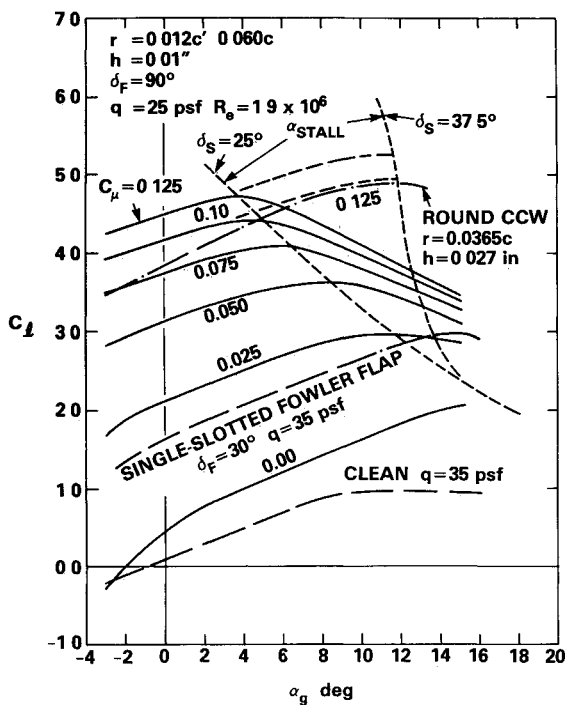


Fig 16 Lift variation with incidence for dual radius CCW configuration B;  $c_f = 0.035c$

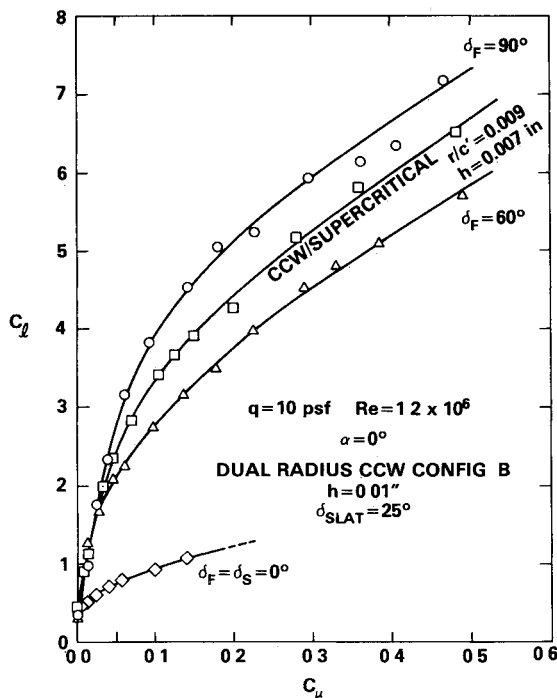


Fig 17 Lift at higher blowing rates,  $\alpha_g = 0$  deg

effect of increased trailing edge radius is emphasized in Fig 11 for the largest dual radius CCW configuration B. The radius just downstream of the slot is 2.67 times that of Fig 10 while the secondary radius is 13.3 times as large. This secondary radius, which is 64% larger than that of the original CCW airfoil of Fig 1, is very effective in turning the jet and enhancing lift. Furthermore, the camber provided by the 90 deg flap deflection adds 0.5 to 0.6 to the unblown lift coefficient. In addition to the increase in lift dual radius configuration B pushes the lift peaks that occurred at  $C_\mu = 0.04$  in Fig 10 up to  $C_\mu = 0.13$  (pressure ratio of 2.2). At angles of attack greater than 3 deg the peaks are minimal or

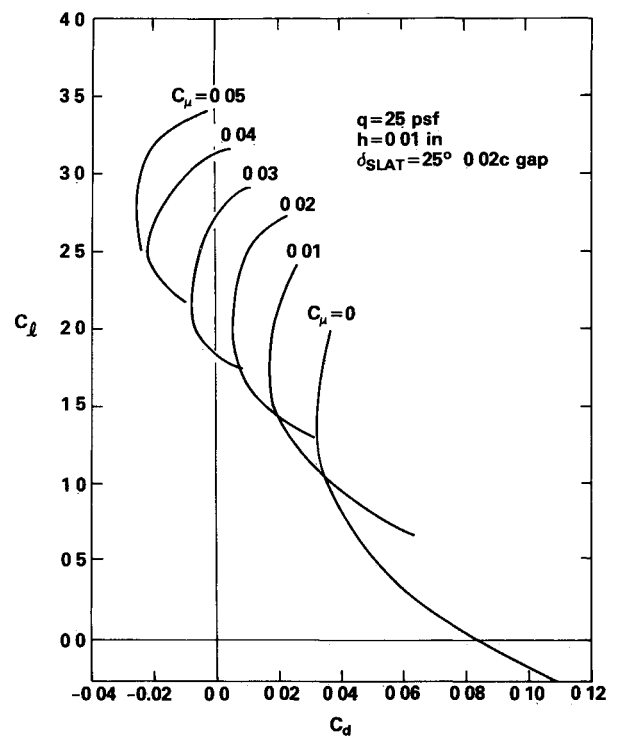


Fig 18 Drag polars at constant blowing for dual radius CCW configuration A;  $c_f = 0.0223c$

nonexistent. Reference 8 data for the CCW/supercritical airfoil indicate that these peaks may be moved to higher  $C_\mu$  by reducing the jet slot height or further increasing the radius. Leading edge stall occurs at high lift and incidence due to insufficient slat deflection.

Reduction in flap deflection reduces the airfoil geometric camber as well as the maximum angle through which the jet may turn. Those effects are shown in Fig 12 for 0 and 60 deg flap deflection. The 0 deg case becomes essentially a 33 deg jet flap, while the 60 deg flap produces 93 deg of jet turning and appreciable lift. The advantages of these two configurations are: 1) lower drag due to reduced projected area and 2) increased jet thrust recovery. The 60 deg flap could thus be effectively employed as a takeoff setting.

The pressure distributions in Fig 13 give further insight into the above discussion. The increased suction peaks produced over the trailing edge radii indicate why the lift is more than tripled by increasing the flap deflection from 0 to 90 deg at  $C_\mu \approx 0.10$ . The  $C_p = -40$  value shows why the larger radii are more effective: they are more able to prevent the high velocity jet from separating from the radius before sufficient turning is produced. The increased suction spike on the slat leading edge points to the nearness of leading edge stall at this slat deflection. Note in this figure, that the slat pressures are plotted normal to the chord rather than deflected, and that the slat is retracted for the 0 deg flap case, since it represents a cruise configuration. The small spike at  $x/c = 0.15$  is due to the exposed cove on the main airfoil into which the slat trailing edge retracts in cruise. The solid symbols are the leading and trailing edges of each separate element.

#### A 6 High Lift Airfoil Comparison

A summary comparison of all the above A 6 high lift configurations is presented in Fig 14 for a typical geometric incidence of 9 deg. The large radius CCW airfoil data from Fig 2 have been adjusted to 25 deg slat deflection as a basis for comparison. Only the two dual radii configurations are superior to the original large configuration in lift, and they fall below its performance at higher  $C_\mu$  because the jet is limited to a maximum turning angle of 123 deg. For the full round large CCW jet turning can continue on to 150 deg or

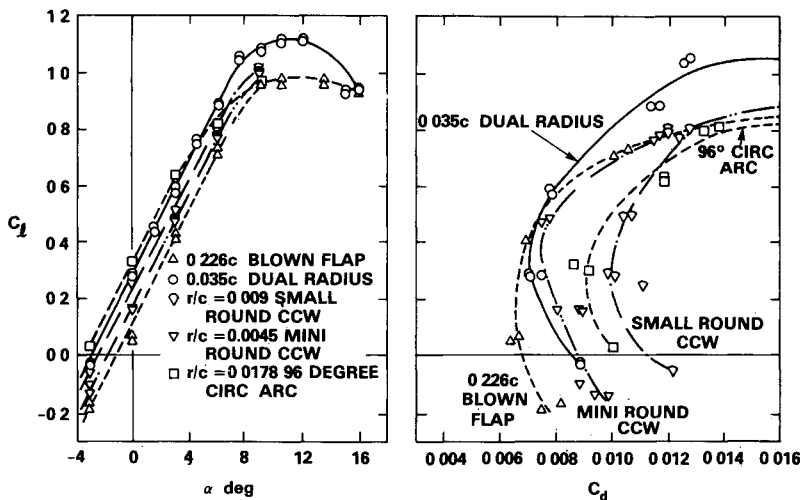


Fig 19 Blowing off clean airfoil comparison

more. However, from a mechanization and drag standpoint this large CCW is impractical and thus most of the configurations shown offer significant operational improvement. To serve as a reference to the actual airplane, the single slotted semi Fowler flap ( $C_F = 0.30c$ ) employed on the A 6 was also tested in connection with the Grumman test of Ref. 10. For  $C_\mu$  in the range of 0.05 or greater, all CCW airfoils tested exceeded the mechanical flap's capability except for the mini radius configuration. A similar comparison is shown in Fig. 15 for  $\alpha_g = 3^\circ$  and includes the 0.226c blown flap configuration.<sup>10</sup> The leading edge stall problem is now avoided at this lower incidence and the dual radius exceeds its Fig. 14 performance at higher blowing. Both the 60 deg dual radius and the 0.226c blown flap behave in the typical blown flap manner; once flow is turned to the flap upper surface angle the lift variation becomes nearly linear with  $C_\mu$  instead of the parabolic function typical of a round CCW. For  $C_\mu > 0.026$  the 90-deg flap dual radius exceeds the 0.226c blown flap lift, even though it is less than one sixth the chord length. The blown flap is superior at low and no blowing due to the extra camber produced by its longer chord length. All three of the CCW configurations can double the lift of the baseline single slotted flap in the  $C_\mu < 0.16$  range; the 0.226c blown flap cannot.

Lift variation with angle of attack is shown in Fig. 16 for the larger flap dual radius CCW and for the 37.5 deg slat configuration from Fig. 2. Clearly, leading edge stall limits  $C_{l_{max}}$  at higher blowing. This is improved considerably by increased slat deflection. With the same 37.5 deg slat, the dual radius configuration offers significantly higher  $C_{l_{max}}$  than the original large radius CCW. For baseline comparison, both the clean A 6 airfoil and the single slotted flap A 6 airfoil data from Ref. 10 ( $Re = 2.2 \times 10^6$ ) are shown.

The effect of extending the available blowing range was investigated by reducing the dynamic pressure to 10 psf so that available pressure and mass flow would yield higher  $C_\mu$ . Figure 17 shows the high lift obtained by the larger chord dual radius CCW in comparison to the CCW/supercritical. Because the secondary radius exceeds that of the supercritical airfoil, so also does the lift. The generation of  $C_l$  approaching 8 at 0 deg incidence appears quite promising, should the increased  $C_\mu$  be available. In these higher blowing ranges lift is nearly a linear function of  $C_\mu$  for either blown flap or full round CCW trailing edge.

#### Drag Variation with Blowing

Drag polars at constant  $C_\mu$  are shown in Fig. 18 for the shorter flap dual radius CCW configuration A, but the trends are similar for the other CCW geometries. In general, for a constant  $\alpha_g$ , increase in  $C_\mu$  results in reduced drag as thrust is recovered from the jet itself. In this figure the initial high

drag levels at low  $C_\mu$  and incidence are due to separated flow on the 90 deg flap and on the slat lower surface (at no blowing and  $\alpha_g = 0^\circ$  it is operating at  $-25^\circ$  local incidence). These data are, of course, two dimensional values and do not address the three dimensional induced drag component due to lift, which will become the dominant drag value for finite wing configurations. Additional drag and pitching moment data are discussed in Ref. 13.

#### Blowing off Comparison

A major design goal of an improved high lift airfoil was to minimize any cruise drag penalty. The various A 6 blown airfoils tested above are compared in their clean configurations in Fig. 19 where slat flap, and circular arc trailing edge are retracted; small and mini CCW trailing edges are left deployed but the slat is retracted. The clean blown flap is considered to be the same configuration as the clean cruise airfoil. As the CCW trailing edge thickness increases, so too does the aft camber and resulting lift due to camber; the 96 deg circular arc shifts the lift curve upwards by an increment of 0.21 over the clean airfoil. Along with this thickness, camber and lift increases cause a corresponding drag increase as shown by the drag polars. The one exception is the dual radius configuration, whose large secondary radius ends in a thin near sharp trailing edge thus avoiding aft surface flow separation. In fact, for  $C_l > 0.5$ , the dual radius yields less drag than the clean airfoil probably because the clean airfoil requires higher angle of attack to reach the same  $C_l$ . Reference 13 also compares these unblown airfoils, with flaps and slats extended, to the large radius original CCW airfoil of Fig. 1. The minimum drag of the unblown 90 deg flap dual radius CCW is about 40% that of the larger radius original CCW and occurs at much higher  $C_l$ . At the same  $C_l$  (say 1.0) the unblown dual radius drag is 25% that of the large radius, and it is less at higher  $C_l$ . In general, the drag levels of these small trailing edges show considerable improvement over those of the original larger trailing edge radius.

#### Conclusions and Recommendations

A series of reduced size CCW trailing edge configurations has been developed and subsonically evaluated in a program to reduce the complexity, size and weight of the CCW high lift system, while maintaining the high lift previously generated and reducing or eliminating the unblown cruise drag penalty of the thick trailing edge. The following conclusions resulted from those investigations:

- 1) A small round trailing edge could be incorporated into the existing aft contour of a thick supercritical airfoil. On this airfoil a radius one fourth the size of the original A 6/CCW

airfoil yielded slightly greater lift than that for 0.036c' radius, producing lift coefficients near 7.0 at  $\alpha = 0$  deg. Furthermore, the large undeflected leading-edge radius of the supercritical airfoil provided the same leading-edge stall prevention as the 37.5-deg slot of the A-6/CCW

2) Base drag was sufficiently reduced by the small trailing-edge radius so that unblown subsonic  $C_d$  was nearly the same as the baseline supercritical airfoil or could be reduced to less than the baseline by a minimal amount of blowing.

3) Of the single-radius CCW configurations applied to the thin A-6 airfoil section, the largest radii produced the greatest lift, as long as there was sufficient arc length to maintain jet turning. Too small a radius produced lift reductions once a certain blowing pressure ratio was reached.

4) The dual-radius CCW provided an effective means to maintain a large radius, sufficient jet turning, and a thin trailing edge for cruise. A 0.035c' flap length dual-radius configuration produced greater lift than the original thick 0.036c' radius A-6/CCW; at  $\alpha_g = 0$  deg,  $C_l$  greater than 7 was generated from  $C_\mu < 0.5$ , compared to the baseline single slotted mechanical flap  $C_l$  of 1.6 at the same incidence.

5) In the clean configuration with no flap deflection, subsonic drag for the dual-radius configuration was nearly the same or slightly less than the A-6 cruise airfoil. Lift due to trailing-edge camber could allow cruise at lower angle of attack, thus resulting in a reduced drag level.

These results suggest the strong potential of two advanced forms of the Circulation Control Wing airfoil: 1) a CCW/supercritical no-moving-parts configuration with no need for a deflecting leading- or trailing-edge device, and transition from the cruise to high-lift modes by initiation of blowing, and 2) a thinner high-performance CCW airfoil with a small-chord dual-radius flap and some type (blown or mechanical) of effective leading-edge device. The flap geometry would provide no cruise penalty (actually the availability of a blowing slot for maneuverability or cruise drag reduction could be quite beneficial), and its larger secondary radius would provide even greater lift than large single-radius configurations. The strength of the dual-radius airfoil lies in its ability to provide a large turning radius, arc length, and jet exit angle accompanied by a very simple conversion to a nearly conventional cruise airfoil.

These data confirm that two families of improved CCW airfoils can, in fact, generate excellent STOL performance with little or no subsonic cruise penalty and without the weight, complexity, and size of conventional mechanical or powered high-lift systems. The remaining unknown is the

effect of the trailing-edge geometries on the airfoil characteristics in high subsonic or transonic flow. This concern will be addressed in transonic two-dimensional wind tunnel investigations now being undertaken as part of the DTNSRDC program for development of these advanced airfoils.

## References

- <sup>1</sup>Englar, R. J., Stone, M. B., and Hall, H., "Circulation Control—An Updated Bibliography of DTNSRDC Research and Selected Outside References," DTNSRDC Rept. 77-0076, Sept. 1977.
- <sup>2</sup>Englar, R. J., Hemmerly, R. A., Moore, W. H., Seredinsky, V., Valckendere, W. G., and Jackson, J. A., "Design of the Circulation Control Wing STOL Demonstrator Aircraft," *Journal of Aircraft*, Vol. 18, Jan. 1981, pp. 51-58.
- <sup>3</sup>Pugliese, A. J. and Englar, R. J., "Flight Testing the Circulation Control Wing," AIAA Paper 79-1791, Aug. 1979.
- <sup>4</sup>Englar, R. J., "Development of the A-6/Circulation Control Wing Flight Demonstrator Configuration," DTNSRDC Rept. ASED-79/01, Jan. 1979.
- <sup>5</sup>Englar, R. J., "Subsonic Two-Dimensional Wind Tunnel Investigations of the High Lift Capability of Circulation Control Wing Sections," DTNSRDC Rept. ASED-274, April 1975.
- <sup>6</sup>Nichols, J. H. Jr., Englar, R. J., Harmis, M. J., and Huson, G. G., "Experimental Development of an Advanced Circulation Control Wing System for Navy STOL Aircraft," AIAA Paper 81-0151, Jan. 1981.
- <sup>7</sup>McGhee, R. H. and Bingham, G. H., "Low-Speed Aerodynamic Characteristics of a 17-percent Thick Supercritical Airfoil Section, Including a Comparison Between Wind-Tunnel and Flight Data," NASA TM X-2571, July 1972.
- <sup>8</sup>Englar, R. J., "Low-Speed Aerodynamic Characteristics of a Small, Fixed-Trailing Edge Circulation Control Wing Configuration Fitted to a Supercritical Airfoil," DTNSRDC Rept. ASED-81/08, March 1981.
- <sup>9</sup>Englar, R. J., "Development of an Advanced No-Moving Parts High-Lift Airfoil," *Proceedings of ICAS/AIAA Aircraft Systems and Technology Conference*, ICAS-82-6.5.4, Aug. 1982, pp. 951-959.
- <sup>10</sup>"Wind Tunnel Test Report-2D NSRDC Test of a 64A008.4 Mod Airfoil, Blown Flaps Phase," Grumman Aerospace Corporation Rept. No. WS-128( )-R-4, Vol. I, Feb. 1983.
- <sup>11</sup>Englar, R. J. and Ottensofer, J., "Calibration of Some Subsonic Wind Tunnel Inserts for Two-Dimensional Airfoil Experiments," DTNSRDC Rept. ASED AL-275, Sept. 1972.
- <sup>12</sup>Englar, R. J., "Two-Dimensional Subsonic Wind Tunnel Test of a Cambered 30-Percent Thick Circulation Control Airfoil," DTNSRDC Rept. ASED AL-201, May 1972.
- <sup>13</sup>Englar, R. J. and Huson, G. G., "Development of Advanced Circulation Control Wing High Lift Airfoils," AIAA Paper 83-1847 July 1983.

## AIAA Meetings of Interest to Journal Readers\*

Date	Meeting (Issue of <i>AIAA Bulletin</i> in which program will appear)	Location	Call for Papers†
Aug 19-25†	<b>XVI International Congress of Theoretical and Applied Mechanics</b>	Lyngby, Denmark	
Aug 20-22	<b>AIAA Guidance and Control Conference (June)</b>	Westin Hotel Seattle, Wash.	Oct. 1983
Aug 20-22	<b>AIAA Atmospheric Flight Mechanics Conference (June)</b>	Westin Hotel Seattle, Wash.	Nov. 1983
Aug 21-23	<b>AIAA 2nd Applied Aerodynamics Conference (June)</b>	Westin Hotel Seattle, Wash.	Oct. 1983
Sept 10-14	<b>14th Congress of the International Council of the Aeronautical Sciences (ICAS)</b>	Toulouse, France	April 1983

\*For a complete listing of AIAA meetings, see the current issue of the *AIAA Bulletin*.

†Issue of *AIAA Bulletin* in which Call for Papers appeared.

‡Co-sponsored by AIAA. For program information, write to: AIAA Meetings Department, 1633 Broadway, New York, N.Y. 10019.